

Dynamic Stability and Levitation Control in Maglev Systems

Peter A. Sayegh*

Columbia University - Department of Electrical Engineering,
500 W 120th St Mudd 1310, New York, NY 10027

Hadrien Déo†

École polytechnique, Institut Polytechnique de Paris, Route de Saclay, 91120 Palaiseau, France

Yazan Abou Rabii‡

Université de Picardie Jules Verne (UPJV), Pôle santé 3,
Rue Des Louvels, 80036 Amiens CEDEX 1, France

Arnaud Couairon§

CPHT, CNRS, École polytechnique, Institut Polytechnique de Paris, Route de Saclay, 91120 Palaiseau, France

This work provides tools for optimizing the stability and levitation of Maglev trains. To optimize passenger capacity, we derive an expression for levitation height as a function of additional weight, refining this model by fitting free parameters to a scaled-down experimental Electromagnetic Suspension (EMS) train. This approach accurately predicts levitation dynamics, with applications toward safer and more efficient Maglev systems and offers groundwork for further stability and load capacity improvements.

I. INTRODUCTION

Imagine a toy train floating effortlessly above its track, defying gravity and gliding smoothly with minimal friction. This captivating phenomenon is the essence of magnetic Levitation (Maglev) technology, which has the potential to revolutionize transportation by enabling high-speed, low-friction travel¹. Maglev trains operate by using magnetic forces to lift and propel vehicles along a guideway, eliminating the need for traditional wheels and rails. This not only reduces mechanical wear but also allows for higher speeds and smoother rides.

A major challenge in Maglev design is achieving stable levitation while maintaining safety and efficiency under varying load conditions. Maglev systems are usually classified into two types: Electromagnetic Suspension (EMS), which relies on attractive magnetic forces for levitation, and Electrodynamic Suspension (EDS), which uses repulsive forces generated by currents induced in conductive guideways^{2,3}. EMS systems require active control to counteract inherent instabilities dictated by Earnshaw's Theorem⁴, but can operate at any speed, whereas EDS systems are passively stable but require minimum speed for levitation. While active stabilization is required in practice and addressed through feedback control in commercial systems, our primary objective is to characterize the relationship between levitation height and applied load.

In this work, we explore the physics of a simplified

EMS system using a combination of experiment and theoretical analysis. A key aim is to demonstrate how fundamental concepts from classical electrodynamics, typically covered in an undergraduate curriculum⁵, can be applied to describe and predict the behavior of Maglev systems. We derive an analytical relationship between the levitation height and the mass added to the train using a magnetic dipole approximation and then validate this model against measurements from a scaled-down experimental train. By comparing theory and experiment, we show how even a reduced-scale system can capture the essential physics of full-scale Maglev trains, making this approach a valuable tool for teaching core electromagnetic principles in a tangible, real-world context. Understanding this load-height relationship is essential for optimizing passenger capacity in commercial Maglev systems.

II. EXPERIMENTAL SETUP

II.1. The Scaled-Down Maglev Train Experiment

A scaled-down Maglev train model was constructed to investigate how the levitation height of the train changes with added mass. The train's base was a wooden block with dimensions of 12 cm (length), 5 cm (width), and 2 cm (height), fitted with Neodymium magnets on its underside. These magnets interacted with magnetic tape laid on the track to achieve levitation. The total mass of the train, including the magnets and wooden block, was $m_0 = 62 \pm 1$ g. The uncertainty in mass measurements is attributed to the precision of the weighing scale used.

The track consisted of a 50 cm strip of magnetic tape attached to a cardboard base, with a width of 8 cm. To

* pas2232@columbia.edu

† hadrien.deo@polytechnique.edu

‡ yazan.abou-rabii.b2022@alumni.polytechnique.org

§ arnaud.couairon@polytechnique.edu

maintain lateral stability, 90-degree angle pieces were affixed to the edges of the track, preventing the train from sliding during experimentation. A key component of the setup was the use of monopolar magnetic tape. Therefore, following the approach used in bonded Nd-Fe-B magnet fabrication depicted by Nlebedim et. al. in 2017, where strong external magnetic fields are applied to align internal domains, we repolarized commercially available bipolar magnetic tape by rubbing it with neodymium magnets.⁶ This method effectively realigns the tape's magnetic domains to form a monopolar strip as required for stable levitation.

The experimental procedure involved gluing two strips of repolarized magnetic tape onto the underside of the train to form the levitating mechanism. Similarly, two long strips of magnetic tape were affixed to the track to act as rails, with the same monopolar alignment. This configuration ensured stable levitation for the experiment.

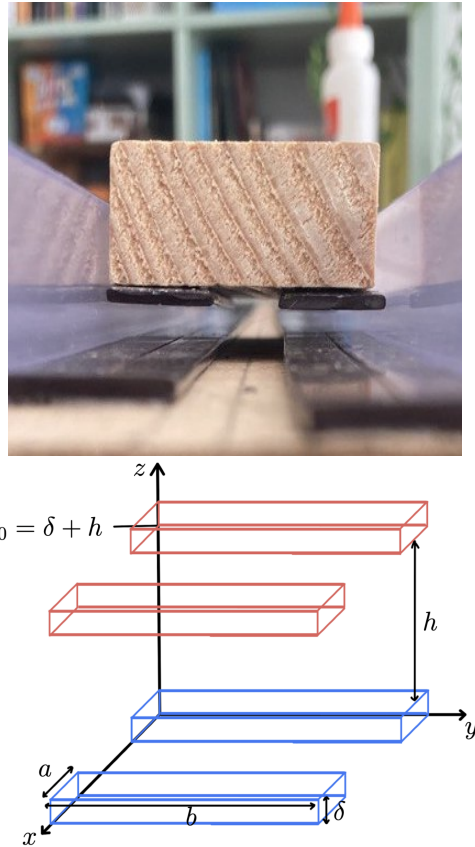


Figure 1. Top: Scaled-down experimental maglev train showing wooden base with neodymium magnets and cardboard cup for additional weights. Bottom: Schematic diagram of experimental geometry showing rail dimensions ($a \times b$), track width, and levitation height measurement setup.

II.2. Measurement of Levitation Height

To study the effect of mass on levitation height, a lightweight cardboard cup was placed on top of the train to hold additional weights. Rice was used as an adjustable weight source, allowing precise increments of mass to be added. The mass of the system was measured using a weighing scale with a precision of 1 g, leading to a measurement uncertainty of $u(m) = \pm 1$ g. Levitation height was measured using a ruler with a resolution of 1 mm, and the corresponding uncertainty was taken as $u(h) = \pm 0.5$ mm, accounting for observer error.

The experimental data for levitation height (h) and mass (m) are summarized in Table I (Appendix A). These measurements formed the basis for further theoretical modeling and analysis.

II.3. Force Derivation and Theoretical Fitting

Maglev systems rely on electromagnetic forces to counteract gravitational forces and achieve stable suspension. The net force on the levitating body can be described as:

$$F_{\text{net}} = F_{\text{mag}} - F_{\text{grav}}, \quad (1)$$

where F_{mag} is the upward magnetic force, and $F_{\text{grav}} = Mg$ is the downward gravitational force, with M being the total mass of the levitating object and g the acceleration due to gravity.

For ensuring equilibrium at a specific levitation height, the system must satisfy:

$$F_{\text{mag}} = F_{\text{grav}}. \quad (2)$$

The relationship between levitation height (h) and added mass (m) was derived by modeling the forces acting on the train. To simplify calculations, we assumed the lower and upper magnets were perfectly aligned, neglecting diagonal forces, and treated the thickness of the magnets as negligible compared to the height of the train. The geometry used in this derivation is shown in Fig. 1.

The magnetic force exerted by the guideway on the train in the vertical direction (z) was computed by considering the magnetic dipole interaction. The magnets were modeled as infinitesimal layers of dipoles with a moment $d\mu = -M dx dy dz \hat{\mathbf{e}}_z$, where M is the magnetization. The force in the z -direction was derived by inte-

grating over all lower and upper dipoles:

$$\begin{aligned}
F(z) = & \frac{2\mu_0 M^2 \delta}{\pi} \frac{1}{a^2 + b^2} \left[z \left(a \sinh^{-1} \left(\frac{a}{z} \right) + b \sinh^{-1} \left(\frac{b}{z} \right) \right. \right. \\
& - a \sinh^{-1} \left(\frac{a}{B(z)} \right) - b \sinh^{-1} \left(\frac{b}{A(z)} \right) \left. \right) \\
& + ab \left(\tan^{-1} \left(\frac{z}{a} \right) - \tan^{-1} \left(\frac{z}{b} \right) \right) \\
& - 2a^2 \tan^{-1} \left(\frac{a(\sqrt{a^2 + b^2 + z^2} - \sqrt{a^2 + b^2})}{z(b + \sqrt{a^2 + b^2})} \right) \\
& \left. \left. - 2b^2 \tan^{-1} \left(\frac{b(\sqrt{a^2 + b^2 + z^2} - \sqrt{a^2 + b^2})}{z(a + \sqrt{a^2 + b^2})} \right) \right] . \quad (3)
\end{aligned}$$

Here, $A(z) = \sqrt{a^2 + z^2}$ and $B(z) = \sqrt{b^2 + z^2}$, and a , b , and δ are the rail's width, length, and thickness, respectively. The detailed derivation of the force is given in Appendix B

The equilibrium condition was determined by balancing the magnetic force with the total gravitational force:

$$F(z) = (m + m_0)g. \quad (4)$$

To validate the model, we fitted the experimental data using a linear regression of the form $\hat{m}_i = p\tilde{F}(z_i) + q$, where p and q are fitting parameters. The results are shown in Fig. 2.

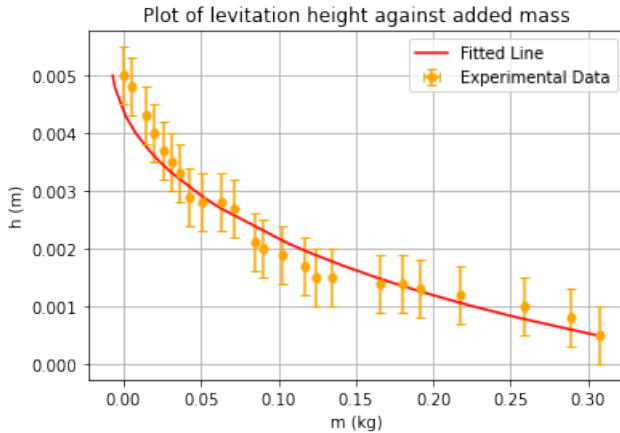


Figure 2. Levitation height as a function of added mass. Experimental data points (orange circles) with error bars show measured heights, and the fitted theoretical curve (red line) represents the analytical model derived from magnetic dipole theory.

The fitted curve closely matches the experimental data, accurately capturing the non-linear decrease in levitation height with increasing mass. This indicates that the model reflects the underlying physical relationships within the experimental uncertainty.

II.4. Application to a real EMS train

Our experiment and theoretical analysis have culminated in significant findings regarding the electromagnetic suspension (EMS) capabilities of the Maglev system.

As seen in Figure 2 the fit is particularly close to the values between 0.03 and 0.30 kg of added mass. However between 0 and 0.4 the data point seem to decrease in a linear way. In fact, for the three first points, the fit gives a value out of the error bars. Finally, after 0.30 kg, we observe a sharp drop in the train's altitude not modeled by our fit, which continues decreasing until it reaches zero but in a convex manner.

We know from the director of Iran Maglev Technology (IMT) Dr. Hamid Yaghoubi's article in the Journal of Engineering that "In EMS system, the vehicle is levitated about 1 to 2 cm above the guideway using attractive forces".⁷ Therefore, we numerically solve $h(m) < h_c = 1\text{cm}$ by taking the parameters of a real train i.e. $a = 0.06\text{m}$, $b = 153\text{m}$, $\delta = 0.0014\text{m}$, and $m_0 = 20 \times 10^3\text{kg}$.

In this configuration, we obtain a critical mass of 7.5×10^4 kg which corresponds to 941 people with an average mass of 80 kg. This result is close to the maximum capacity of the Shanghai EMS Maglev train, i.e. 959 passengers according to China Discovery,⁸ which may serve as a validation of the model when adjusted to reflect practical conditions, confirming that the theoretical predictions can indeed mirror practical outcomes when all relevant factors are considered.

III. RESULTS AND DISCUSSION

To quantitatively assess the accuracy of our fit in predicting levitation heights based on varying masses, we calculate the coefficient of determination, denoted R^2 , which yields an accuracy score of 96.0%. This result is encouraging, yet certain regions reveal limitations in the fit's effectiveness.

However, the high uncertainty in the data, mainly due to the 1 mm uncertainty of the ruler used for measurement, complicates the evaluation of the fit's correspondence with the observed data.

Regarding the accuracy of our fit, we approximated the system by assuming negligible forces between diagonal magnets and considering all four magnets to be identical. Since the experiment itself was an approximation of a maglev train, our fit cannot fully capture the train's behavior, especially under conditions where the assumptions of the system become inadequate—such as when the train is in close proximity to the guideway.

Then as a limitation to our model and fit, we found that the fit diverges from the experimental data in the interval $(0, 0.03)\text{ kg}$ and for values above 0.30 kg . The linear behavior of the data points under 0.03 kg of added

mass can be understood by noting that $m \ll m_0$, so the change in height induced by adding m to the train will result in a change in height $z \ll z_0$. If $H(m)$ is the true function giving the height of the train as a function of m , close to 0 we have

$$H(m) = h_0 + m \frac{dh}{dm},$$

which indicates that the height of the train decreases linearly with the added mass. However, this is not accounted for by our fit, as the function F does not depend on the mass.

Similarly, for masses higher than 0.3 kg, the height decreases sharply. This suggests a maximum in the magnetic force, beyond which the gravitational force prevents the train from levitating. Once again, this behavior is not captured by our fit. Firstly, it was derived under the assumption that the magnets are composed of infinitesimal magnetic dipoles. Two magnetic dipoles create a force that goes to infinity when they get closer. In our case since the dipole are infinitesimal they create a force with finite maximum but which still increases drastically when the magnets are pulled together, thus explaining the convex profile of our fit. Secondly, we assumed that the height of the train is much larger than the thickness of the magnet, which is not true for $m > 0.3\text{kg}$.

Analysis of the force gradient reveals a critical distinction between our experimental model and real EMS systems. Figure 3 shows the force $\tilde{F}(z)$ and its derivative $d\tilde{F}/dz$ for our scaled-down model. Throughout the operating range, we observe $d\tilde{F}/dz > 0$, indicating that our system exhibits passive stability—vertical perturbations naturally generate restoring forces without requiring active control.

However, this positive gradient exposes a fundamental limitation in extrapolating our findings to real EMS trains. The theorem established by Samuel Earnshaw in 1842 states that it is impossible for a static arrangement of charges or magnets to achieve stable equilibrium through purely electrostatic or magnetostatic forces⁴. Our experimental system circumvents this theorem by utilizing *repulsive* magnetic forces (monopolar magnetic tape with like poles facing each other), which are inherently stable. In contrast, real EMS systems employ *attractive* electromagnetic forces between electromagnets on the vehicle and ferromagnetic rails on the guideway.

For an attractive magnetic system, the stability criterion becomes:

$$\frac{\partial F_{\text{mag}}}{\partial z} < 0, \quad (5)$$

where a negative gradient is required. If the train moves

upward (decreasing z), the attractive force must increase to pull it back down; conversely, if it moves downward (increasing z), the force must decrease. This configuration is inherently unstable and necessitates continuous

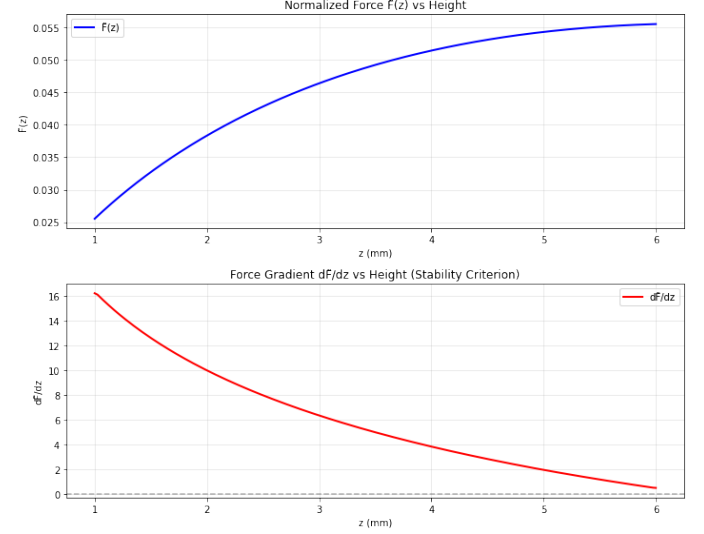


Figure 3. Force function $\tilde{F}(z)$ and force gradient $d\tilde{F}/dz$ for the experimental model. The positive derivative throughout indicates passive stability characteristic of repulsive magnetic systems.

active feedback control, with electromagnet currents adjusted thousands of times per second to maintain stable levitation.

A comprehensive model of real EMS dynamics would require: (1) inverting the force direction to model attractive rather than repulsive interactions, (2) incorporating the U-shaped electromagnet geometry surrounding the guideway, (3) including time-varying currents and feedback control algorithms, and (4) accounting for dynamic effects such as vibrations and aerodynamic forces. Nevertheless, our simplified model provides valuable pedagogical insight into the electromagnetic principles governing magnetic levitation systems and offers a tractable framework for understanding levitation capacity constraints.

SUPPLEMENTARY MATERIAL

Please see the supplementary material for the code and data used in our simulations at github.com/peter-sayegh/maglev.git.

AUTHOR DECLARATIONS

The authors have no conflicts to disclose.

- ¹ H-W Lee, K-C Kim, and J Lee. Review of maglev train technologies. *IEEE Transactions on Magnetics*, 42(10):1917–1925, 2006.
- ² BV Jawayant. Electromagnetic suspension and levitation. *Rep. Prog. Phys.*, 44:411–472, 1973. URL <https://iopscience.iop.org/article/10.1088/0034-4885/44/4/002/pdf>.
- ³ Luning Hao, Zhen Huang, Fangliang Dong, Derong Qiu, Boyang Shen, and Zhijian Jin. Study on electrodynamic suspension system with high-temperature superconducting magnets for a high-speed maglev train. *IEEE Transactions on Applied Superconductivity*. doi: 10.1109/TASC.2018.2881688.
- ⁴ Samuel Earnshaw. On the nature of the molecular forces which regulate the constitution of the luminiferous ether. *Transactions of the Cambridge Philosophical Society*, 7:97–112, 1842.
- ⁵ David J. Griffiths. *Introduction to Electrodynamics*. Cambridge University Press, 5th edition, 2024.
- ⁶ I. C. Nlebedim, Huseyin Ucar, C. B. Hatter, R. W. McCallum, M. P. Paranthaman, M. S. Kesler, J. Ormerod, and et al. Studies on in situ magnetic alignment of bonded anisotropic nd-fe-b alloy powders. *Journal of Magnetism and Magnetic Materials*, 422:168–173, 2017. doi: 10.1016/j.jmmm.2016.08.090.
- ⁷ Hamid Yaghoubi. The most important maglev applications. *Journal of Engineering*, 2013:Article ID 537986, 1–19, 2013. doi:10.1155/2013/537986. URL <https://doi.org/10.1155/2013/537986>.
- ⁸ China Discovery. Shanghai maglev train. <https://www.chinadiscovery.com/shanghai/shanghai-maglev.html>, 2023.

Appendix A: Experimental Data

Table I. Experimental data for the mass (m) and levitation height (h) of the Maglev train model. The uncertainties are ± 1 g for m and ± 0.5 mm for h .

m (g)	0	5	15	20	26	31	36	43	51	63
h (mm)	5.0	4.8	4.3	4.0	3.7	3.5	3.3	2.9	2.8	2.8
m (g)	71	85	90	103	117	124	135	166	180	192
h (mm)	2.7	2.1	2.0	1.9	1.7	1.5	1.5	1.4	1.4	1.3
m (g)	217	259	289	307	322					
h (mm)	1.2	1.0	0.8	0.5	0.0					

Appendix B: Analytical Derivation of the Force Induced by the Dipole Moment

In this section, we derive the expression for the magnetic force $F(z)$ acting on a Maglev train system, modeled as layers of magnetic dipoles.

We model each rail as a continuous surface distribution of magnetic dipoles. Let M be the surface magnetization of the rail, oriented along the z -axis. The infinitesimal

dipole moment of an element of the rail is defined as:

$$d\mu = M dx' dy' \hat{z},$$

The objective is to calculate the magnetic force between two layers of dipoles (representing the upper and lower rails) as a function of the distance z between them.

The magnetic vector potential \mathbf{A} at a point $\mathbf{r} = (x, y, z)$ due to an infinitesimal surface dipole element located at $\mathbf{r}' = (x', y', 0)$ is given by:

$$d\mathbf{A}(\mathbf{r}) = \frac{\mu_0 M}{4\pi} \frac{d\mu \times (\mathbf{r} - \mathbf{r}')}{|\mathbf{r} - \mathbf{r}'|^3}$$

$$d\mathbf{A}(\mathbf{r}) = \frac{\mu_0 M}{4\pi} \frac{dx' dy'}{[(x - x')^2 + (y - y')^2 + z^2]^{3/2}} \begin{bmatrix} -(y - y') \\ x - x' \\ 0 \end{bmatrix},$$

where μ_0 is the permeability of free space ($\mu_0 = 4\pi \times 10^{-7} \text{ N/A}^2$).

To find the total vector potential generated by the lower rail of width a and length b , we integrate over the entire surface of the bottom rail:

$$\mathbf{A}(\mathbf{r}) = \frac{\mu_0 M}{4\pi} \int_{x-a}^x \int_{y-b}^y \frac{dX dY}{[X^2 + Y^2 + z^2]^{3/2}} \begin{bmatrix} -Y \\ X \\ 0 \end{bmatrix}.$$

where we did the change of variable $X = x - x'$, $Y = y - y'$.

We derive the integrals necessary to calculate the magnetic potential and force in the system. The integrals will be evaluated over the specified ranges using the correct variables dX and dY .

$$I_0(X) = \int_{y-b}^y \frac{Y dY}{(X^2 + Y^2 + z^2)^{3/2}} = \left[\frac{1}{\sqrt{X^2 + Y^2 + z^2}} \right]_{Y=y-b}^y$$

$$I_1(Y) = \int_{x-a}^x \frac{X dX}{(X^2 + Y^2 + z^2)^{3/2}} = \left[\frac{1}{\sqrt{X^2 + Y^2 + z^2}} \right]_{X=x-a}^x.$$

$$I_2 = \int_{x-a}^x I_0(X) dX = \left[\ln \left(\frac{\sqrt{X^2 + Y^2 + z^2} + X}{\sqrt{X^2 + (y-b)^2 + z^2} + X} \right) \right]_{X=x-a}^x.$$

$$I_3 = \int_{y-b}^y I_1(Y) dY = \left[\ln \left(\frac{\sqrt{(x-a)^2 + Y^2 + z^2} + Y}{\sqrt{x^2 + Y^2 + z^2} + Y} \right) \right]_{Y=y-b}^y.$$

From there, one gets the full expression of the vector potential $\mathbf{A}(\mathbf{r})$:

$$\mathbf{A}(\mathbf{r}) = \frac{\mu_0 M}{4\pi} \begin{cases} \ln \left(\frac{\sqrt{(y-b)^2 + z^2 + (x-a)^2} + (x-a)}{\sqrt{(y-b)^2 + z^2 + x^2} + x} \right) \frac{\sqrt{y^2 + z^2 + x^2} + x}{\sqrt{y^2 + z^2 + (x-a)^2} + (x-a)} \\ \ln \left(\frac{\sqrt{(y-b)^2 + z^2 + x^2} + (y-b)}{\sqrt{y^2 + z^2 + x^2} + y} \right) \frac{\sqrt{y^2 + z^2 + (x-a)^2} + y}{\sqrt{(y-b)^2 + z^2 + (x-a)^2} + (y-b)} \end{cases} \hat{z}.$$

The magnetic field \mathbf{B} can be derived from the vector potential \mathbf{A} using the relation:

$$\mathbf{B} = \nabla \times \mathbf{A}.$$

However, due to the symmetry of the system, only the z -component of the magnetic field is significant for our analysis. Thus, we focus on calculating B_z , which is given by:

$$B_z = \frac{\partial A_y}{\partial x} - \frac{\partial A_x}{\partial y}.$$

The upper rail, placed at a height z , consists of a layer of dipole moments aligned downward:

$$d\mu = -M dx dy \hat{z}.$$

The force on each dipole in the presence of a magnetic field is given by:

$$d\mathbf{F} = \nabla(d\mu \cdot \mathbf{B}).$$

To find the total force on both upper rails by both lower rails, we integrate over its surface. The z -component of the force is:

$$F(z) = -2M \int_0^a \int_0^b \partial_z B_z(z) dx dy.$$

$$F(z) = -2M \int_0^a dx \int_0^b \partial_z (\partial_x A_y - \partial_y A_x) dy.$$

$$F(z) = -2M \frac{\partial}{\partial z} \left(\int_0^b [A_y]_{x=0}^a dy - \int_0^a [A_x]_{y=0}^b dx \right).$$

Using the identities:

$$\sinh^{-1}(U) = \ln(\sqrt{1+U^2} + U)$$

and

$$\int_0^{U_m} \sinh^{-1}\left(\frac{U}{U_0}\right) dU = U_m \sinh^{-1}\left(\frac{U_m}{U_0}\right) - \sqrt{U_0^2 + U_m^2} + U_0$$

we obtain the following expression of the induced force along the z -axis:

$$F(z) = -\frac{2\mu_0 M^2}{\pi} \frac{\partial \Phi}{\partial z}(z)$$

where Φ , defined below, is a dimensionless potential for the force:

$$\begin{aligned} \Phi(z) &= a \sinh^{-1}\left(\frac{a}{z}\right) + b \sinh^{-1}\left(\frac{b}{z}\right) - a \sinh^{-1}\left(\frac{a}{B(z)}\right) \\ &\quad - b \sinh^{-1}\left(\frac{b}{A(z)}\right) - 2(A(z) + B(z)) + 2(z + \sqrt{a^2 + b^2 + z^2}) \end{aligned} \quad (B1)$$

With $A(z) = \sqrt{a^2 + z^2}$ and $B(z) = \sqrt{b^2 + z^2}$

To extend our results to a more realistic 3D scenario, we consider the finite thickness δ of the upper rail. The magnetic field correction can be approximated as:

$$F^{(3D)}(z) \propto \frac{\partial B_z^{(3D)}}{\partial z} \approx B_z^{(2D)}(z + \delta) - B_z^{(2D)}(z).$$

This approximation accounts for the finite thickness of the magnetic layers and provides a more accurate representation of the force. We proceed as follows:

First, we consider an elementary dipole moment $d\mu = -M_{3D} dx dy dz \hat{z}$ where $M_{3D} = \frac{M_{2D}}{\delta}$ is the magnetization in A/m, which can be defined as the density of dipole moments per unit volume.

$$\mathbf{F} = 2 \int_0^a \int_0^b \int_{z_0}^{z_0+\delta} \nabla(d\mu \cdot \mathbf{B}).$$

Since we are only interested in F_z by symmetry, we proceed as follows:

$$F_z(z) = -2M_{3D} \int_0^a \int_0^b \int_{z_0}^{z_0+\delta} B_z^{(3D)}(z) dx dy dz.$$

Expanding further, using the above approximation:

$$F_z = -2M_{3D} \int_{z_0}^{z_0+\delta} \int_0^b \int_0^a \left(\frac{\partial}{\partial z} \int_0^\delta B_z^{(2D)}(z - z') dz' \right) dx dy dz.$$

$$F_z = \frac{1}{\delta} \int_{z_0}^{z_0+\delta} dz \int_z^{z-\delta} dz' \left(\int_0^a \int_0^b -2M \partial_z B_z^{(2D)}(z) dx dy \right).$$

On the other hand, we recognize the force expression we had using the zero-thickness model (i.e. in two dimensions):

$$F_z^{(2D)} = -2 \int_0^b \int_0^a M_{2D} dx dy \partial_z B_z^{(2D)}(z).$$

Thus:

$$F_z = \frac{1}{\delta} \int_{z_0}^{z_0+\delta} dz \int_{z-\delta}^z \left[F_z^{(2D)}(z') \right] dz'.$$

$$F_z = -\frac{2\mu_0 M_{3D}^2 \delta}{\pi} \int_{z_0}^{z_0+\delta} dz \int_{z-\delta}^z \left[\frac{\partial \Phi}{\partial z}(z') \right] dz'.$$

Given a position z_0 below the top rail, we have:

$$F_z(z_0) = -\frac{2\mu_0 M_{3D}^2 \delta}{\pi} \int_{z_0}^{z_0+\delta} (\Phi(z - \delta) - \Phi(z)) dz$$

We define the primitive Ψ of Φ :

$$\Psi(z) = \int \Phi(z) dz.$$

Step-by-Step Derivation:

$$J_0 = \int a \sinh^{-1}\left(\frac{a}{z}\right) dz.$$

$$J_0 = a z \sinh^{-1}\left(\frac{a}{z}\right) + a^2 \ln\left(z + \sqrt{a^2 + z^2}\right).$$

$$J_1 = \int b \sinh^{-1}\left(\frac{b}{z}\right) dz.$$

$$J_1 = b z \sinh^{-1}\left(\frac{b}{z}\right) + b^2 \ln\left(z + \sqrt{b^2 + z^2}\right).$$

$$J_2 = \int -a \sinh^{-1}\left(\frac{a}{B(z)}\right) dz.$$

$$J_2 = -a z \sinh^{-1}\left(\frac{a}{B(z)}\right) + 2a^2 \arctan\left(\frac{z}{\sqrt{a^2 + b^2}}\right).$$

$$J_3 = \int -b \sinh^{-1}\left(\frac{b}{A(z)}\right) dz.$$

$$J_3 = -b z \sinh^{-1}\left(\frac{b}{A(z)}\right) + 2b^2 \arctan\left(\frac{z}{\sqrt{a^2 + b^2}}\right).$$

$$J_4 = \int -2(A(z) + B(z)) dz$$

$$\begin{aligned} J_4 = & - \left[z\sqrt{a^2 + z^2} + a^2 \sinh^{-1}\left(\frac{z}{a}\right) \right] \\ & - \left[z\sqrt{b^2 + z^2} + b^2 \sinh^{-1}\left(\frac{z}{b}\right) \right]. \end{aligned} \quad (\text{B2})$$

$$J_5 = \int 2\left(z + \sqrt{a^2 + b^2 + z^2}\right) dz$$

$$J_5 = z^2 + z\sqrt{a^2 + b^2 + z^2} + (a^2 + b^2) \sinh^{-1}\left(\frac{z}{\sqrt{a^2 + b^2}}\right).$$

So, by combining all terms, the final expression for $\Psi(z)$ is:

$$\begin{aligned} \Psi(z) = & a z \sinh^{-1}\left(\frac{a}{z}\right) + b z \sinh^{-1}\left(\frac{b}{z}\right) \\ & - a z \sinh^{-1}\left(\frac{a}{B(z)}\right) - b z \sinh^{-1}\left(\frac{b}{A(z)}\right) \\ & - z\sqrt{a^2 + z^2} - a^2 \sinh^{-1}\left(\frac{z}{a}\right) \\ & - z\sqrt{b^2 + z^2} - b^2 \sinh^{-1}\left(\frac{z}{b}\right) \\ & + z^2 + z\sqrt{a^2 + b^2 + z^2} + (a^2 + b^2) \sinh^{-1}\left(\frac{z}{\sqrt{a^2 + b^2}}\right). \end{aligned} \quad (\text{B3})$$

Hence, we obtain an expression of F_z the force induced by the magnetic dipole moment on the top rails along the z-axis:

$$F_z(z_0) = \frac{2\mu_0 M_{3D}^2 \delta}{\pi(a^2 + b^2)} (\Psi(z_0 + \delta) + \Psi(z_0 - \delta) - 2\Psi(z_0))$$

Then, we generalize to an arbitrary position z between the two rails, drop the 2D/3D indices, consider $\delta/z \ll 1$ and find:

$$\begin{aligned} F(z) = & \frac{2\mu_0 M^2 \delta}{\pi} \frac{1}{a^2 + b^2} \left[z \left(a \sinh^{-1}\left(\frac{a}{z}\right) + b \sinh^{-1}\left(\frac{b}{z}\right) \right. \right. \\ & - a \sinh^{-1}\left(\frac{a}{B(z)}\right) - b \sinh^{-1}\left(\frac{b}{A(z)}\right) \left. \right) \\ & + ab \left(\tan^{-1}\left(\frac{z}{a}\right) - \tan^{-1}\left(\frac{z}{b}\right) \right) \\ & - 2a^2 \tan^{-1}\left(\frac{a(\sqrt{a^2 + b^2 + z^2} - \sqrt{a^2 + b^2})}{z(b + \sqrt{a^2 + b^2})}\right) \\ & \left. - 2b^2 \tan^{-1}\left(\frac{b(\sqrt{a^2 + b^2 + z^2} - \sqrt{a^2 + b^2})}{z(a + \sqrt{a^2 + b^2})}\right) \right]. \end{aligned} \quad (\text{B4})$$